Energy Proceedings
Vol 58, 2025
ISSN 2004-2965

Decoding Multiscale Carbon Emission Dynamics: A Systematic Framework Leveraging Land Use Patterns and Explainable Artificial Intelligence

Haizhi Luo [1], Yubo Liu [1], Xia Song [2], Xinyu Gao [1], Yiwen Zhang [3], Xiaohu Yang [1,*], Xiangzhao Meng [1,*]

1 Institute of the Building Environment & Sustainability Technology, School of Human Settlements and Civil Engineering, Xi'an Jiaotong University, Xi'an 710049, China

2 Shaanxi Zhongwei Energy Technology, Xi'an, 712000, China

3 School of Architecture and Civil Engineering, Xiamen University, Xiamen 361005, China
* Corresponding Author: xiaohuyang@xjtu.edu.cn (Yang X.); xzmeng@xjtu.edu.cn (Meng X.)

ABSTRACT

Carbon emissions are a key driver of global climate change, and their accurate characterization and prediction are essential for promoting regional sustainable development. This study develops a novel carbon emission modeling framework that integrates interpretable machine learning with land use data, without dependence on socio-economic indicators. This allows for emission prediction beyond the decoupling stage and captures spatial distribution patterns with high accuracy and interpretability. The Yangtze River Delta region is used as a case study. By combining Geographic Information System-based kernel density analysis for land-use refinement with an optimized Extra Trees Regression model, the approach achieves high predictive performance (R^2 = 0.86 for testing set). Model interpretability is enhanced using Shapley Additive exPlanations, which reveal nonlinear effects of various land types on emissions. Future land use scenarios are simulated using the Optimized Land Expansion Analysis Strategy and a Cellular Automaton based on Multiple Random Seeds, achieving overall accuracy above 85%. Projections estimate total carbon emissions in the Yangtze River Delta will reach 1,581 million tons by 2030, with Shanghai and Suzhou contributing 224 and 172 million tons, respectively. County-level emissions are further examined using spatial econometric models, which identify a significant clustering pattern (Moran's *I* = 0.61). As industrial land becomes more dispersed, emission hotspots shift toward regional centers.

Keywords:
Carbon emission; Land use; Interpretable machine learning; Multi-scale characterization; Dynamic prediction

1. INTRODUCTION

Global climate change constitutes one of the most pressing and immediate environmental challenges confronting the world [1]. Greenhouse gas (GHG) emissions, particularly carbon emissions, have driven a persistent increase in the Earth's average temperature [2], which in turn has triggered a cascade of severe climate impacts [3], including more frequent extreme weather events, rising sea levels, accelerated glacier retreat, and ecological degradation [4].

Accurately understanding and quantifying GHG emissions, especially carbon emissions across regions and sectors, is essential for developing effective climate policies and advancing emission reduction efforts [5]. Such efforts form the basis for regional authorities to devise carbon mitigation plans and strategies [6]. Therefore, research on carbon emission characterization and prediction is of substantial importance from both methodological and applied perspectives.

2. MATERIALS AND METHODS

2.1 Search site

The construction of urban clusters is driving global development, but it also causes a lot of GHG emissions [6]. The Yangtze River Delta (YRD) region, encompassing Shanghai and adjacent provinces (Jiangsu, Zhejiang, and Anhui), represents one of China's most dynamic and economically vibrant areas [7]. YRD is situated in eastern China, with the Yangtze River flowing through it. YRD region covers an area of 358,000 km² and a permanent population of 235 million in 2021 [8]. With generated a GDP of 27.6 trillion RMB, the YRD region has become one of the largest urban agglomerations in China and the world.

This is a paper for the 11th Applied Energy Symposium: Low Carbon Cities & Urban Energy Systems (CUE2025), July 18-22, 2025, Kitakyushu, Japan.

In general, as a growth pole of global socio-economic development [9], the YRD region faces many environmental challenges. The empirical and methodological research on carbon emission characterization and prediction in this region can provide a global demonstration for carbon emission reduction and sustainable development.

2.2 Research material

The study integrates a range of geographic and panel data to support land-use subdivision, land-use expansion analysis, and carbon emission accounting. Land use/land cover (LULC) data [10], along with POIs from the A-map platform, are utilized for detailed land-use type subdivision. Driving factors of LUEX include DEM (CAS), road vectors (OSM), nighttime lights (GEE), meteorological data (CAS, [11]), and socio-economic indicators such as GDP and population. Satellite imagery supports the calculation of LST and NDVI, while carbon emissions by sector (industrial, commercial, residential, etc.) are sourced from CCG for emission estimation [12].

2.3 Model and method

This study comprises four main steps: (1) Data Pre-processing, where statistical and vector data (e.g., GDP, population, POIs) are interpolated and rasterized to construct a unified dataset including land-use subdivisions, expansion drivers, and emission data; (2) Model Training & Interpretation, where land-use areas are used to predict carbon emissions via machine learning, with Shapley Additive exPlanations (SHAP) used for interpretability and R^2, MRE for evaluation; (3) LEAS Modeling, where a random forest-based LEAS model predicts land expansion using socio-environmental drivers, evaluated by RMSE and OOB RMSE; (4) Emission Simulation, where a Markov model estimates land demand, and combined outputs are used for spatially explicit emission prediction, evaluated by Overall Accuracy and Kappa.

3. MODEL CONSTRUCTION AND VALIDATION

The Extra Trees model was optimized via grid search and evaluated with cross-validation (R^2 train = 0.99, R^2 test = 0.86). Statistical tests (t-test, PCC = 0.98, $p < 0.001$) and residual diagnostics confirmed accuracy and robustness. Minor bias in extreme values is acceptable given known uncertainties in carbon accounting [13].

The LEAS model showed low RMSE (< 0.10) and acceptable OOB RMSE (< 0.15), with slight deviations for cropland and forest due to sampling limitations. Given the study's focus on built-up areas, the model performance meets requirements.

CARS simulations based on LEAS outputs yielded high accuracy (Kappa = 0.89/0.94; OA = 0.94/0.96 for 2015/2020). Lower 2015 accuracy is likely due to data limitations. Built-up area prediction is prioritized, and ecological land trade-offs are acceptable.

4. RESULT

4.1 Impact of land-use area on carbon emissions

Ecological land types generally exhibit carbon sink effects. Fig 1 shows that plowland, woodland, and grassland negatively correlate with carbon emissions, while water bodies have a weak positive effect. However, these effects depend on scale; small ecological patches may act as net emitters due to surrounding anthropogenic activities. Threshold effects were observed—carbon sink capacity becomes significant only when land areas surpass specific thresholds. These findings align with IPCC and related empirical studies [14].

Built-up areas act as carbon sources [15], with complex, often nonlinear impacts. Urban residential and commercial lands exhibit S-curve relationships with carbon emissions, where contributions intensify beyond certain area thresholds (e.g., residential > 86 km²). Mixed-use land shows a strong linear relationship (R^2 = 0.95), with significant emissions increase beyond 53 km². Other urban lands follow a similar pattern, while rural residential land presents inconsistent effects, likely due to heterogeneous energy structures. Industrial land contributes significantly to emissions even at small scales, with rapid increases below 71 km², stabilizing afterward—indicating the need for context-specific industrial land planning.

4.2 Prediction of land use expansion

Land expansion in the YRD is driven by both natural and socio-economic factors [16]. Northern areas, with flat terrain and high solar radiation, favor cropland and industrial development, while the south, with higher precipitation and steeper slopes, supports woodland and grassland expansion. Socio-economically, major cities like Shanghai, Nanjing, and Hangzhou act as growth poles, with dense transportation and service facilities driving built-up land expansion.

The contributions of various factors to land use expansion are shown in Fig 2. The ecological land expansion is mainly influenced by precipitation,

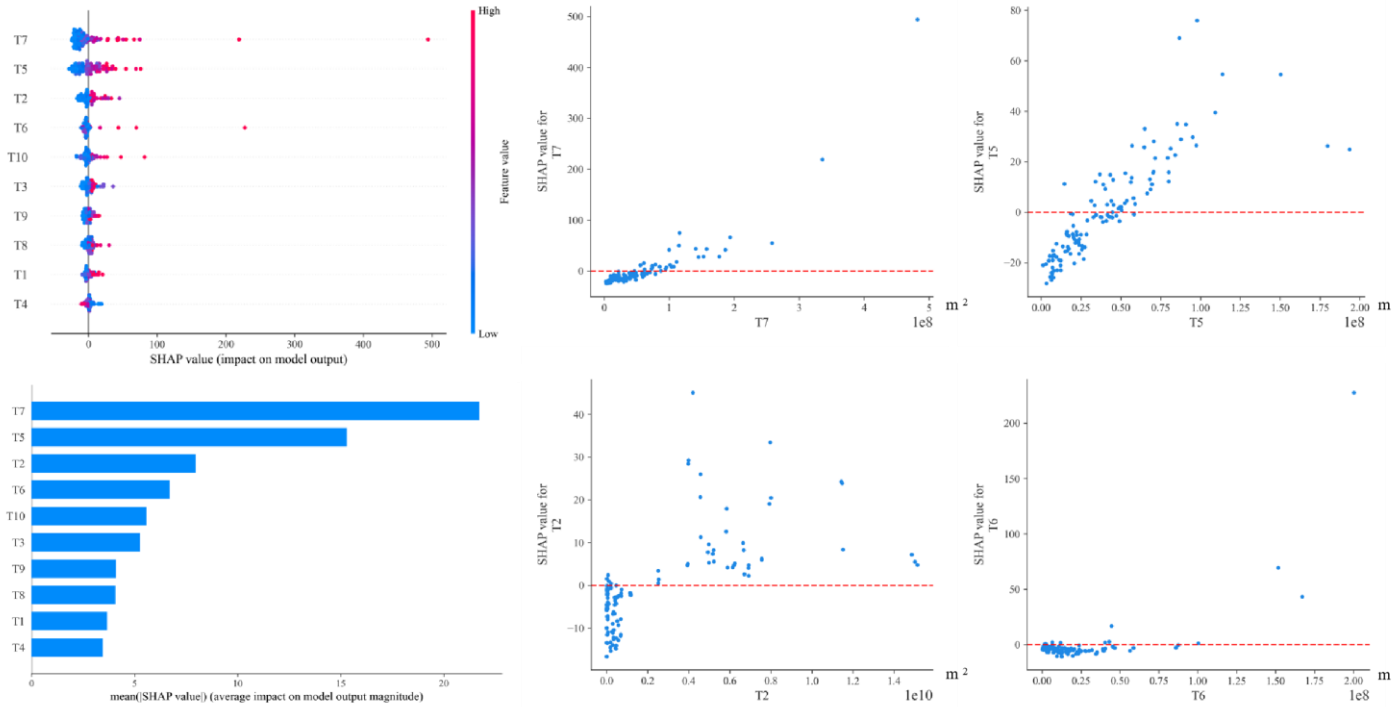

Fig. 1 Impact of land use on carbon emission

temperature, and sunshine hours. Built-up land types are more closely linked to infrastructure and population: residential and commercial land are driven by traffic and service facilities, mixed-use land by GDP and population, and industrial land by transportation nodes and solar energy availability.

Cropland expansion is feasible across most of the region except in dense urban areas, while woodland and grassland are more suitable for southern zones. Residential and commercial land are concentrated in urban centers such as Suzhou and Ningbo, with mixed-use development in megacities like Shanghai and Hangzhou. Expansion patterns vary regionally—northern cities exhibit concentric growth, while eastern cities expand along transport and water corridors. Industrial and transportation land are primarily suited to coastal and central-northern areas.

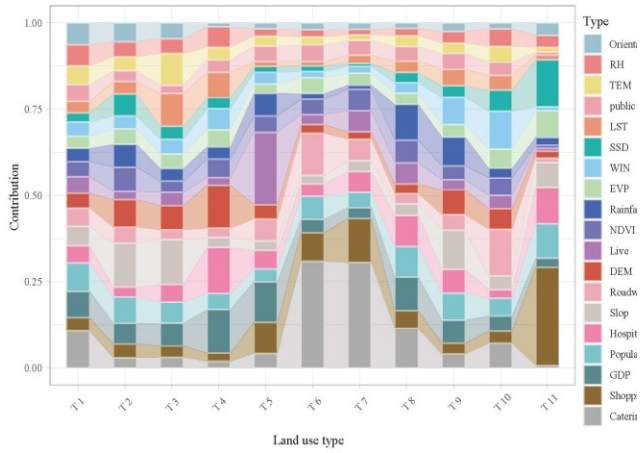

Fig. 2 Contributions of factors to land expansion

4.3 Carbon emission prediction

4.3.1 Regional and City-Scale Emission Projections

Under current development trends, total carbon emissions in the YRD are projected to reach 1,452.61 Mt in 2025 and 1,580.70 Mt in 2030, marking an increase of 207.91 Mt from 2020 levels. Shanghai and Jiangsu are expected to remain relatively stable, while emissions in Zhejiang and Anhui will continue to grow. By 2030, emissions in Zhejiang are projected to rise by 27.71% and in Anhui by 16.24% compared to 2020.

At the city scale, as shown in Fig 3, Shanghai (224 Mt), Suzhou (172 Mt), Wuxi (121 Mt), and Nanjing (121 Mt) will exceed 120 Mt by 2030. High emissions in Changzhou and Wuxi are largely driven by land-intensive industries such as equipment and electronics manufacturing.

Shanghai, Suzhou, and Huainan—are projected to reduce emissions over the next decade due to industrial restructuring and relocation. Shanghai's emissions are expected to drop by 20 Mt, while neighboring cities like

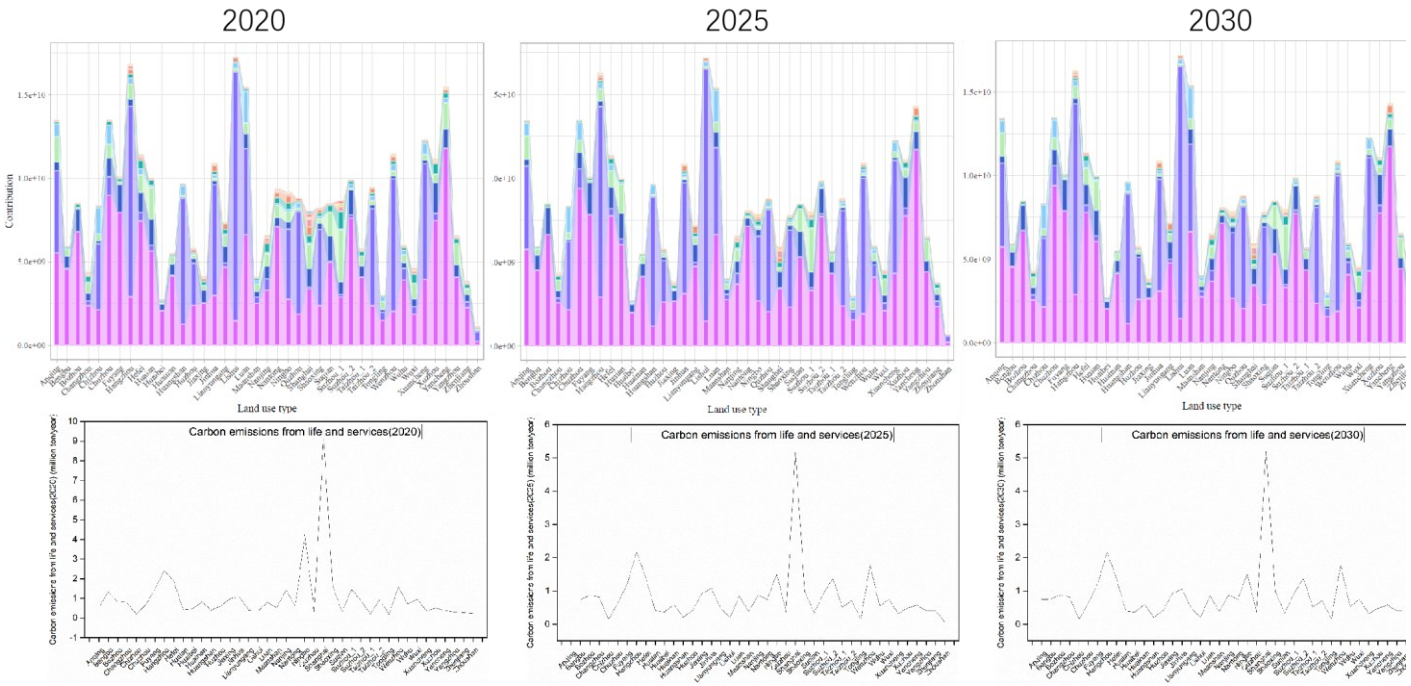

Fig. 3 Characterization and Prediction of city-level carbon emissions

Nantong will face emission increases (e.g., +46 Mt) due to industrial land transfer.

4.3.2 County-Level Carbon Emission Projections

As shown in Fig 4, by 2030, central YRD counties will dominate emissions. Suzhou Industrial Park is projected to emit 31.93 Mt, with Jiangyin, Wujin, Gusu, and Kunshan each exceeding 24 Mt, reflecting their industrial intensity.

In contrast, southern and western counties (e.g., Liandu, Qingtian, Huangshan) are projected to emit < 1.5 Mt due to agricultural dominance and terrain-constrained urbanization.

Districts in Shanghai, such as Pudong, Minhang, and Songjiang, are expected to see significant reductions (>10 Mt each), driven by industrial relocation and compact urban development. However, emissions will rise in surrounding districts (e.g., Jiangyin +7.14 Mt, Wujin +9.16 Mt) and in rapidly developing urban areas like Shushan District, Hefei (+12.45 Mt) due to the expansion of high-tech industrial parks.

4.3.3 Spatial Characteristics of Carbon Emissions

Strong and persistent spatial autocorrelation in YRD carbon emissions (Global Moran's $I > 0.6$, $p < 0.001$), suggesting significant spatial clustering.

As shown in Fig 4, from 2010 to 2020, carbon emission hotspots expanded from the eastern coast to the central YRD, forming a high-emission belt. In the next decade, this belt is expected to shift inland, with the eastern region gradually detaching, and the southwestern regions forming low-emission clusters. Strategic relocation of high-energy-consuming land to these areas could mitigate pressure in central urban zones.

Fig 4 identifies spatial hot and cold spots. High-emission hotspots are concentrated in Suzhou (e.g., Wuzhong), Nanjing, and Wuxi (e.g., Binhu, Huishan). Cold spots are located in less industrialized counties such as Chizhou, Huangshan, and Anqing (e.g., Shitai County, Huangshan District).

5. DISCUSSION

Under the current development trajectory, carbon emissions in the YRD are expected to reach 1,453 Mt by 2025 and 1,581 Mt by 2030, reflecting a 208 Mt increase from 2020. While emissions in Shanghai and Jiangsu are projected to remain relatively stable, Zhejiang and Anhui are anticipated to experience continuous growth, with Zhejiang increasing by 28 % and Anhui by 16 % compared to 2020. By 2030, Shanghai (224 Mt), Suzhou (172 Mt), Wuxi (122 Mt), and Nanjing (121 Mt) will be the major emitters. High emissions in Changzhou and Wuxi are closely linked to the concentration of equipment and electronics manufacturing [17].

Some cities—such as Shanghai, Suzhou, and Huainan—are projected to achieve emission reductions over the next decade due to industrial restructuring and

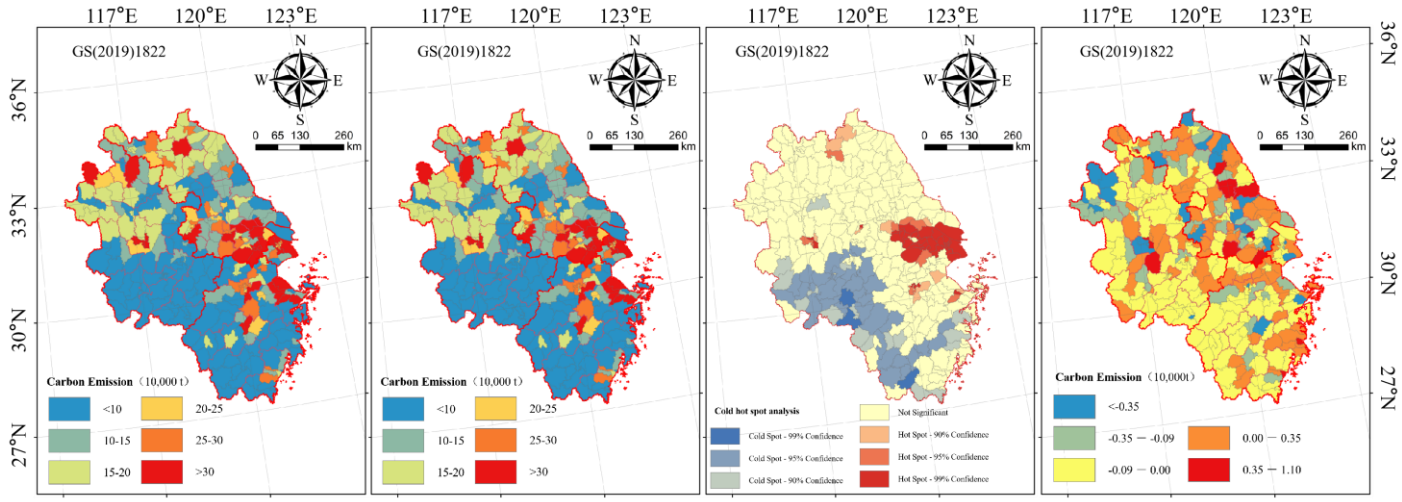

(a) Prediction results of CRCEs at district and county level (2025)

(b) Prediction results of CRCEs at district and county level (2030)

(c) Analysis of spatial cold and hot spots of carbon emission

(d) Carbon emission change at county level (2025-2030)

Fig. 4 Analysis of the spatial statistical characteristics of carbon emissions

land-use adjustments, with Shanghai reducing by 20 Mt and Suzhou by 18 Mt. However, this has driven emissions up in adjacent areas [18], such as Nantong, which is expected to see a 46 Mt increase.

At the county level, emission hotspots are concentrated in industrialized areas of central YRD, with Suzhou Industrial Park reaching 31.93 Mt and several districts (e.g., Jiangyin) exceeding 24 Mt. In contrast, counties in the southern and western YRD—such as Liandu, Qingtian, and Huangshan—are projected to remain below 1.5 Mt due to limited industrial activity and terrain constraints [19]. Within Shanghai, several districts are expected to achieve notable reductions, each exceeding 10 Mt, due to the relocation of high-energy industries and compact development strategies. Surrounding districts, including Jiangyin, Wujin, and Shushan, are expected to see considerable emission increases driven by industrial expansion [20].

Spatially, emissions in the YRD exhibit strong and persistent clustering (Moran's $I > 0.6$, $p < 0.001$, [21]). From 2010 to 2020, emission hotspots expanded from the eastern coastal areas to the central region. Over the next decade, this pattern is expected to shift, with the central region forming the dominant emission core, and the south and west developing low-emission clusters.

Relocating high-emission industries to these lower-value zones could help alleviate environmental pressures in core urban areas [22]. Hotspot analysis reveals that districts in Suzhou, Nanjing, and Wuxi will remain major contributors, while areas in Chizhou, Huangshan, and Anqing are identified as emerging cold spots.

6. CONCLUSIONS

To meet the technical demands of carbon emission characterization and prediction, this study develops a model integrating land-use subdivision with interpretable machine learning. By relying solely on land-use data, the model avoids dependence on socio-economic indicators and supports medium- to long-term forecasting. Land-use subdivision enhances spatial precision, while optimized variable selection in LEAS and CARS enables efficient, large-scale, multi-class land-use prediction. The incorporation of the SHAP algorithm improves model interpretability, offering practical insights for regional carbon reduction strategies, especially within land-use planning frameworks.

Applied to 41 cities in the YRD from 2010 to 2020, the model reveals the marginal impact of different land-use types on carbon emissions and forecasts emissions at multiple administrative scales for 2025 and 2030.

Nevertheless, limitations remain. Future work should expand the study area and extend the temporal coverage to improve model robustness. A more detailed sectoral disaggregation of emissions (e.g., industrial, commercial, residential, agricultural) and refined land-use classification would enable more accurate and granular emission characterization.

ACKNOWLEDGEMENT

This study is supported by *the Fundamental Research Funds for the Central Universities* (xzy022025044). We also express our gratitude to *the Graduate School of Xi*

'an Jiaotong University for its support and funding for our participation in this conference.

REFERENCE

[1] Sonter LJ, Barrett DJ, Moran CJ, Soares-Filho BS. Carbon emissions due to deforestation for the production of charcoal used in Brazil's steel industry. Nature Climate Change. 2015;5:359-363.

[2] Calvo Buendia E, Tanabe K, Kranjc A, Jamsranjav B, Fukuda M, Ngarize S. 2019 Refinement to the 2006 IPCC Guidelines for National Greenhouse Gas Inventories. Geneva, Switzerland, 2019. https://www.ipcc-nggip.iges.or.jp/public/2019rf/.

[3] Gao J, Bukovsky MS. Urban land patterns can moderate population exposures to climate extremes over the 21st century. Nat Commun. 2023;14:6536.

[4] Newman R, Noy I. The global costs of extreme weather that are attributable to climate change. Nat Commun. 2023;14:6103.

[5] Luo H, Li Y, Gao X, Meng X, Yang X, Yan J. Carbon emission prediction model of prefecture-level administrative region: A land-use-based case study of Xi'an city, China. Applied Energy. 2023;348:121488.

[6] Nakhli MS, Shahbaz M, Ben Jebli M, Wang S. Nexus between economic policy uncertainty, renewable & non-renewable energy and carbon emissions: Contextual evidence in carbon neutrality dream of USA. Renew Energy. 2022;185:75-85.

[7] National Development and Reform Commission of China. Implementation plan for carbon peaking in urban and rural construction in China. Beijing, China, 2024. https://www.mohurd.gov.cn/gongkai/zhengce/zhengcefilelib/202207/20220713_767161.html.

[8] Statistics NBo. Statistical Bulletin of the National Economic and Social Development of the People's Republic of China in 2024. Beijing, China, 2024. https://www.stats.gov.cn/sj/zxfb/202502/t20250228_1958817.html.

[9] Li W, Cui Y, Qin Y, Qin H, Dong J. Construction land allocation in Beijing-Tianjin-Hebei and Yangtze River Delta urban agglomerations. J Geogr Sci. 2025;35:501-520.

[10] Xu X, Liu J, Zhang S, Li R, Yan C, Wu S. Remote sensing data set of multi-period land use monitoring in China. Data Center for Resources and Environmental Sciences, Chinese Academy of Sciences. Beijing, China, 2023. https://www.resdc.cn/data.aspx?DATAID=360.

[11] Xu X. Monthly spatial interpolation data set of meteorological elements in China. Data Center for Resources and Environmental Sciences, Chinese Academy of Sciences. Beijing, China, 2023. https://www.resdc.cn/DOI/DOI.aspx?DOIid=104.

[12] Cai B, Dong J, Lei Y, Cao L, Zhang L, Lv C, et al. China city carbon dioxide emissions dataset (2010-2020). China City Greenhouse Gas Working Group. Ministry of Ecology and Environment of the People's Republic of China, 2022. https://www.cityghg.com/pages/database.

[13] Eggleston HS, Buendia L, Miwa K, Ngara T, Tanabe K. IPCC 2006 Guidelines for National Greenhouse Gas Inventories. Hayama, Japan, 2006. https://www.ipcc-nggip.iges.or.jp/public/2006gl/index.html.

[14] Lee H, Calvin K, Dasgupta D, Krinner G, Mukherji A, Thorne P, et al. Climate Change 2023 Synthesis Report. Switzerland, 2023. https://www.ipcc.ch/report/ar6/syr/.

[15] Liu J, Pei X, Zhu W, Jiao J. Multi-scenario simulation of carbon budget balance in arid and semi-arid regions. J Environ Manage. 2023;346:119016.

[16] Luo H, Zhang Y, Gao X, Liu Z, Meng X, Yang X. Multi-scale electricity consumption prediction model based on land use and interpretable machine learning: A case study of China. Advances in Applied Energy. 2024;16:100197.

[17] Luo H, Wang C, Li C, Meng X, Yang X, Tan Q. Multi-scale carbon emission characterization and prediction based on land use and interpretable machine learning model: A case study of the Yangtze River Delta Region, China. Applied Energy. 2024;360:122819.

[18] Chen X, Di Q, Jia W, Hou Z. Spatial correlation network of pollution and carbon emission reductions coupled with high-quality economic development in three Chinese urban agglomerations. Sust Cities Soc. 2023;94:104552.

[19] Shen L, Zhong Z, Chen C, Zhang S, Zhen F. City Network Evolution Characteristics of Smart Industry: Evidence from Yangtze River Delta, China. Chin Geogr Sci. 2024;34:829-848.

[20] Yin H, Xiao R, Fei X, Zhang Z, Gao Z, Wan Y, et al. Analyzing "economy-society-environment" sustainability from the perspective of urban spatial structure: A case study of the Yangtze River delta urban agglomeration. Sust Cities Soc. 2023;96:104691.

[21] Ai M, Chen X, Yu Q. Spatial correlation analysis between human disturbance intensity (HDI) and ecosystem services value (ESV) in the Chengdu-Chongqing urban agglomeration. Ecol Indic. 2024;158:111555.

[22] Lin B, Atsagli P, Dogah KE. Ghanaian energy economy: Inter-production factors and energy substitution. Renew Sust Energ Rev. 2016;57:1260-1269.